Identification of Parameters to correctly adapt Energy-Based Hysteresis Models regarding Rotational Losses

L. Domenig[1], K. Roppert[1], A. Gschwentner[1], A. Sauseng[1], and M. Kaltenbacher[1]
[1] Institute of Fundamentals and Theory in Electrical Engineering, TU Graz, Graz, Austria, lukas.domenig@tugraz.at

The parameter identification of energy-based hysteresis models is extremely important regarding the accuracy of simulation results of, e.g., electrical machines and transformers. This paper aims to propose an extended version to existing parameter identification techniques in order to correctly depict rotational losses up to high saturation levels. On the basis of measurements obtained by a rotational single sheet tester (RSST), the measured magnetic field strength is split into its reversible and irreversible part. Using this information the parameters of an adapted vector hysteresis model are identified by means of a least squares minimization. The model results are compared to the measurements and show a good agreement concerning the vanishing rotational losses at saturation level and the behaviour of the magnetic flux density.

***Index Terms*—Energy-based vector hysteresis, rotational magnetization, rotational losses, hysteresis measurement**

I. Introduction

TO FURTHER improve highly optimized electrical devices such as transformers or electrical machines, the simulation tools used should be able to correctly describe local magnetic properties. Concerning this matter, one main challenge are rotational losses, which can only be determined if the simulation tool can handle local hysteretic effects. State-of-the-art vector hysteresis models are, e.g., so-called energy-based hysteresis (EB) models [1], [2]. To solve real life problems using EB models, the parameters have to be identified for each specific material. To perform this task highly efficient methods exist ([3],[4]), but all approaches lack the ability to correctly describe rotational losses, which are defined as

$$w_{\text{rot}} := \int_0^{2\pi} \|\boldsymbol{b}(\boldsymbol{h})\| \|\boldsymbol{h}\| \sin\theta \, \mathrm{d}\alpha \, . \tag{1}$$

In (1) $\boldsymbol{b}$ is the magnetic flux density, $\boldsymbol{h}$ the field intensity, θ the angle between those two quantities and α is the angle of $\boldsymbol{h}$ compared to a reference direction. Measurements show that the rotational losses are vanishing if the material is in saturation, which is not true for the original EB model. In this paper, the parameters of the EB model are identified using unidirectional measurements and an already existing method to identify its parameters. Then an adaptation is used to consider rotational losses which parameters are identified by means of a splitting of the measured field intensity into its reversible and irreversible part ($\boldsymbol{h} = \boldsymbol{h}_{\text{rev}} + \boldsymbol{h}_{\text{irr}}$) by restating it as a minimization problem and utilizing numerical optimization to solve it.

II. RSST Measurements

The measurements are carried out using a RSST that is shown in Fig. 1, and the tested material is a $80\,\text{mm} \times 80\,\text{mm} \times 1.2\,\text{mm}$ non-oriented steel sheet. To measure the $\boldsymbol{h}$-field, a 3D Hall sensor is employed. For the $\boldsymbol{b}$-field, two coils in x- and y-direction are used. Since the aim is to purely measure losses due to hysteresis, the frequency is kept very low ($f = 1\,\text{Hz}$) to avoid any noticeable influences regarding eddy currents. In Fig. 2 and 3, the results of the measurements for the rotational and for the uniaxial case are shown respectively. They consist of $M = 24$ magnetic field strength levels with its corresponding magnetic flux density values in the rotational case and for the uniaxial case in x-direction. In the uniaxial case, only the major loop is shown to emphasize the anhysteretic curve, calculated from this loop. The measurements are later used to conduct the parameter identification, validate the model results, and to perform the splitting of the magnetic field into its reversible and irreversible part.

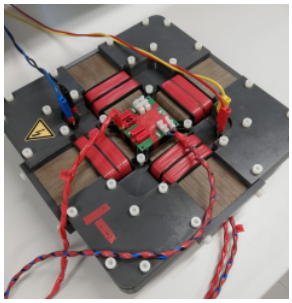

Fig. 1: Rotational single sheet tester used for measurements

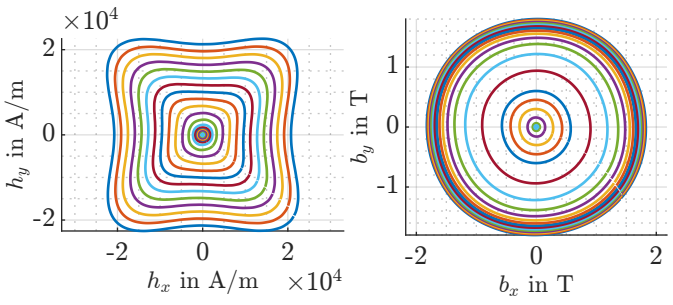

Fig. 2: b_y/b_x and h_y/h_x for increasing magnetic field levels

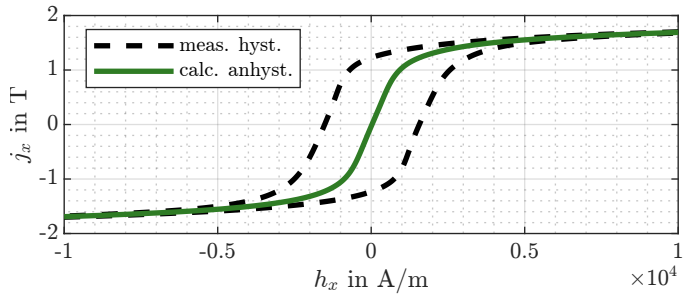

Fig. 3: Measured hysteresis curve and from this curve calculated anhysteresis curve for the uniaxial case

III. Energy-Based Hysteresis Model

In a magnetic sense, the conservation of energy can be written as [5]

$$\dot{u} + d = \boldsymbol{h} \cdot \dot{\boldsymbol{j}} \ , \tag{2}$$

where u is the internal energy, d the dissipation power that is entirely converted into heat, $\boldsymbol{h}$ the applied magnetic field strength and $\boldsymbol{j}$ the resulting magnetic polarization. The used material law can be stated as

$$\boldsymbol{j} = \boldsymbol{b} - \mu_0 \boldsymbol{h} \ , \tag{3}$$

where μ_0 is the vacuum permeability. To enforce ferromagnetic characteristics to the model, the functionals u and d have to be expressed accordingly. The internal energy is the actual energy that is done by the applied field and is for this reason a reversible process. Therefore, only a reversible part $\boldsymbol{h}_{\mathrm{rev}}$ of the magnetic field can contribute, which defines the anhysteretic curve of the material $\mathscr{J}_{\mathrm{an}}(\boldsymbol{h}_{\mathrm{rev}})$. This energy functional can then be expressed as

$$u(\boldsymbol{j}) = \int_0^{\|\boldsymbol{j}\|} \mathscr{H}_{\mathrm{rev,an}}(x) \, \mathrm{d}x \ , \tag{4}$$

where $\mathscr{H}_{\mathrm{rev,an}}$ is the inverse of the anhysteretic function. The second functional describes the dissipation, and therefore, only an irreversible field $\boldsymbol{h}_{\mathrm{irr}}$ can contribute to this power. It is analogically defined by the Coulomb friction that should model the friction that hinders the motion of Bloch walls. This can be described by the expression

$$d := \kappa |\dot{\boldsymbol{j}}| \ , \tag{5}$$

where κ is the pinning force that has to be overcome in order to allow a change in the polarization. To now find an equilibrium, (2) is differentiated w.r.t $\dot{\boldsymbol{j}}$ and set to zero. On the first term, this differentiation yields

$$\boldsymbol{h}_{\mathrm{rev}} = \frac{\partial u(\boldsymbol{j})}{\partial \boldsymbol{j}} \ . \tag{6}$$

The second term is, due to the magnitude function, not differentiable at $\dot{\boldsymbol{j}} = \boldsymbol{0}$. However, it is a convex function and for this reason the concept of a subgradient can be used to define a set $\mathscr{A}$ that gathers all possible gradients

$$\mathscr{A} = \begin{cases} \boldsymbol{h}_{\mathrm{irr}}, \|\boldsymbol{h}_{\mathrm{irr}}\| \leq \kappa & \text{if } \dot{\boldsymbol{j}} = \boldsymbol{0} \\ \boldsymbol{h}_{\mathrm{irr}} = \kappa \boldsymbol{e}_{\dot{\boldsymbol{j}}} & \text{if } \dot{\boldsymbol{j}} \neq \boldsymbol{0} \ . \end{cases}$$

Using these two expressions, the equilibrium equation that governs the behaviour of the model is

$$\boldsymbol{h} - \boldsymbol{h}_{\mathrm{rev}} = \boldsymbol{h}_{\mathrm{irr}} \in \mathscr{A} \ . \tag{7}$$

It determines the irreversible field $\boldsymbol{h}_{\mathrm{irr}}$ in the set $\mathscr{A}$, which is analogous to the behaviour of a spring-friction slider, where the elongation corresponding to the polarization of the spring, is only allowed to change if the friction force of the slider is overcome. An efficient solution strategy of this equation is described in [6]. To increase the accuracy of the model, not only one pinning force is considered, but rather a discrete volumetric weighted distribution of k so-called pseudoparticles that all have an assigned value for their weight ω^k and pinning force κ^k. This helps to better represent the statistical distribution of the impurities that create pinning centres in the ferromagnetic material.

A. Issue of the Model regarding Rotational Losses

Measurements show that for a rotating applied field the losses vanish in saturation of the material. This means that the dissipation of the system goes towards zero, since all magnetic domains are aligned with the applied field and no delay between the $\boldsymbol{b}$-field and the $\boldsymbol{h}$-field occurs. The EB model uses (5) as an expression for the dissipation. In the case of uniaxial excitation, the behaviour of vanishing losses in saturation is enforced by the anhysteretic curve in (4), since in saturation the polarization does not change any more and the dissipation becomes zero. In contrast to that, in the rotational case the polarization always changes in the direction, so $\dot{\boldsymbol{j}}$ is never zero and for this reason the dissipation cannot vanish. This phenomenon of the model can be seen in Fig. 4.

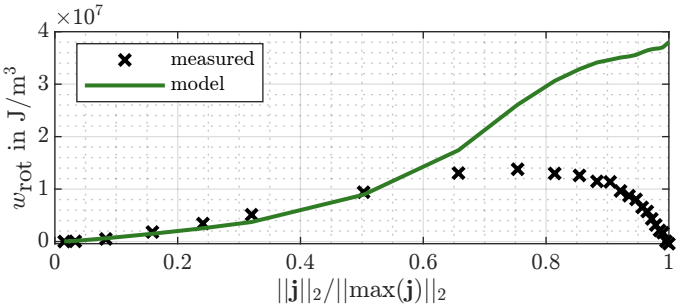

Fig. 4: Comparison of modelled and measured rotational losses

B. Adaptation: Direct Angle Correction

To correct this unphysical behaviour, a possible improvement to the model might be an adaptation of the angle $\theta_{\boldsymbol{h}_{\mathrm{rev}},\boldsymbol{h}}$ between the reversible field and the applied field depending on the state of saturation [7]. This can be done by defining a rotation matrix $\boldsymbol{R}^k$

$$\boldsymbol{R}^k(\phi^k) = \begin{bmatrix} \cos(\phi^k) & -\sin(\phi^k) \\ \sin(\phi^k) & \cos(\phi^k) \end{bmatrix} \ , \tag{8}$$

that rotates the reversible field towards the applied field for every pseudoparticle k and is governed by the following heuristic function,

$$\phi^k = f^k(\|\boldsymbol{j}^k\|)\theta^k_{\boldsymbol{h}^k_{\mathrm{rev}},\boldsymbol{h}^k} = \left(\frac{\|\boldsymbol{j}^k\|}{j_{\mathrm{sat}}}\right)^{\nu^k} \theta^k_{\boldsymbol{h}^k_{\mathrm{rev}},\boldsymbol{h}^k} \ , \tag{9}$$

where ν^k is a design parameter that has to be chosen properly to fit the behaviour of the material. The angle ϕ^k that has to be rotated is the current angle $\theta_{\boldsymbol{h}_{\text{rev}},\boldsymbol{h}}$ for full saturation ($\|\boldsymbol{j}\| = j_{\text{s}}$). This results in a vanishing phase lag between the magnetic field strength and the flux density due to an aligning of the reversible and applied magnetic field, and therefore no power is dissipated. This lets the rotational losses drop to zero according to its description by (1). The function $f^k(\|\boldsymbol{j}^k\|)$ can also be chosen differently, as long as it has the same characteristics as the used one in this work. In Fig. 5 this rotation can be seen for low and high magnetic field strengths.

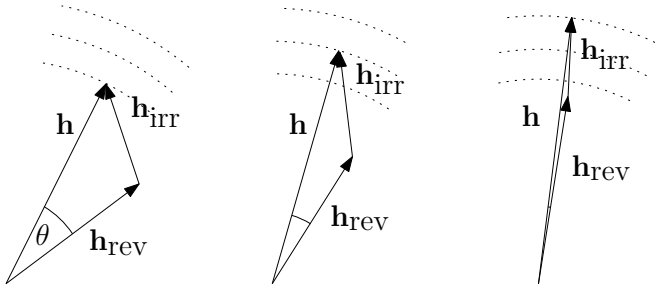

Fig. 5: Correction of the angle for different levels of the magnetic field strength

IV. Splitting of the Measured Magnetic Field Strength

To obtain information about how the reversible and the irreversible part of the measured magnetic field behave in order to identify ν^k, a splitting of these quantities is proposed. The polarization $\boldsymbol{j}$ is known from the measured fields by using the material law (3) and $\boldsymbol{j}$ always points in the direction of $\boldsymbol{h}_{\text{rev}}$, which is defined by the choice of the expression of the internal energy in (4). Exploring this relation, the magnitude of the reversible part can be obtained by solving for each time step t_k

$$\|\boldsymbol{h}_{\text{rev}}(t_k)\| = \underset{\|\boldsymbol{h}_{\text{rev}}(t_k)\|}{\arg\min} \quad \|\mathscr{J}_{\text{an}}(\|\boldsymbol{h}_{\text{rev}}(t_k)\|) - j^{\text{meas}}(t_k)\|_2 \ , \tag{10}$$

where $j^{\text{meas}}(t_k)$ is the magnitude of the measured polarization for the current time step t_k and $\mathscr{J}_{\text{an}}(\|\boldsymbol{h}_{\text{rev}}\|)$ is the anhysteretic function obtained by uniaxial measurements of the sample. Then the reversible part can be obtained by multiplying the magnitude by the current normalized direction vector of the polarization $\boldsymbol{e}_j$

$$\boldsymbol{h}_{\text{rev}} = \|\boldsymbol{h}_{\text{rev}}\|\boldsymbol{e}_j \tag{11}$$

and the irreversible part is evaluated by using

$$\boldsymbol{h}_{\text{irr}} = \boldsymbol{h} - \boldsymbol{h}_{\text{rev}} \ , \tag{12}$$

where $\boldsymbol{h}$ is known by the measurements. Using this technique, the actual phase lag $\theta_{\boldsymbol{h}_{\text{rev}},\boldsymbol{h}}$ between the reversible part and the magnetic field can be used to adapt the EB model such that the rotational losses are depicted properly. The contribution of all field components for an increasing excitation can be seen in Fig. 6 and the measured angle in Fig. 7. It can be recognized that the angle indeed vanishes. However, the reversible part of the field does not dominate near saturation. For this reason, an adaptation via an angle correction might be better suited than making the irreversible field vanish directly [8].

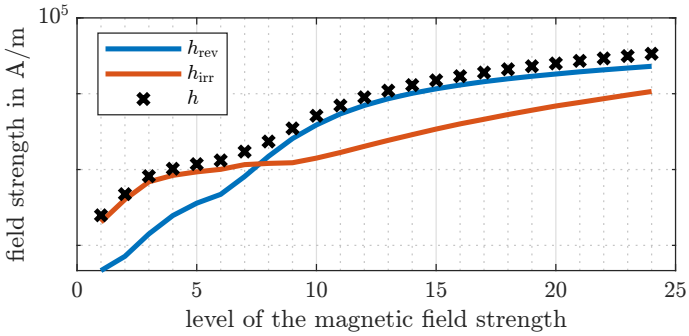

Fig. 6: Obtained reversible and irreversible part of the magnetic field strength by applying the splitting

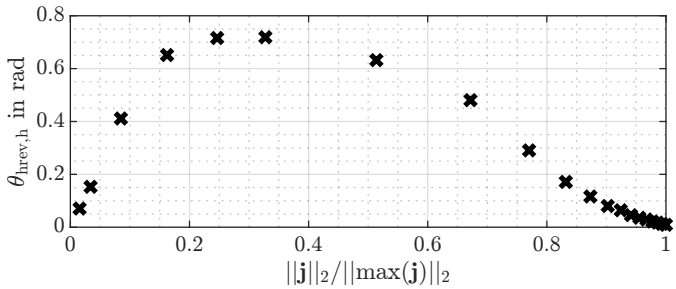

Fig. 7: Obtained angle from the splitting between the measured magnetic field strength and reversible field

V. Proposed Parameter Identification

The parameter identification of the EB model is done in three steps. First, the anhysteretic function $\mathscr{J}_{\text{an}}(\|\boldsymbol{h}_{\text{rev}}\|)$ is calculated using the major loop of the hysteresis curve. To use this behaviour in the EB model an analytical function for example using the arctan(), the tanh(), the Langevin or the double Langevin can be used. The parameter of the chosen function can be identified via a least squares minimization. However, in this work a spline interpolation of the measurements is performed to be independent of analytical functions, that are not capable to match every material perfectly. The second step is to identify the set of weights and pinning forces (ω^k, κ^k). They are obtained by using the method introduced in [9], where a method is described that is able to derive the pinning field probability density function $\omega(\kappa)$ from uniaxial measurements. This distribution is then discretized using k pseudoparticles to obtain a value for every weight and pinning force. The last step is to identify the parameter ν^k for each pseudoparticle (see (9)) to get the function $f^k(\|\boldsymbol{j}^k\|)$ such that $\theta_{\boldsymbol{h}_{\text{rev}},\boldsymbol{h}}$ matches the measured characteristics. This is done by restating the identification as a minimization problem. As an objective function, the following least squares error between the measured and simulated angles is used

$$\nu = \underset{\nu\in[1,\infty)^N}{\arg\min} \sum_{l=1}^{M} (\theta_{\boldsymbol{h}_{\text{rev}},\boldsymbol{h},\text{meas},l} - \theta_{\boldsymbol{h}_{\text{rev}},\boldsymbol{h},\text{sim},l}(\nu))^2 \ , \tag{13}$$

where M is the number of measured magnetic field levels. This problem is solved via a proper numeric optimization algorithm. In this case, the function *fminunc()* from MATLAB [10] is used. The results concerning the angle $\theta_{\boldsymbol{h}_{\text{rev}},\boldsymbol{h}}$, rotational losses w_{rot} and the $\boldsymbol{b}$-field can be seen in Fig. 8, 9 and 10, respectively. They show that by using the information of the measured angle $\theta_{\boldsymbol{h}_{\text{rev}},\boldsymbol{h}}$ it is possible to choose ν^k such that the simulated rotational losses match the characteristics of the measured one, and the simulated magnetic flux density fits the measured one with some minor deviations.

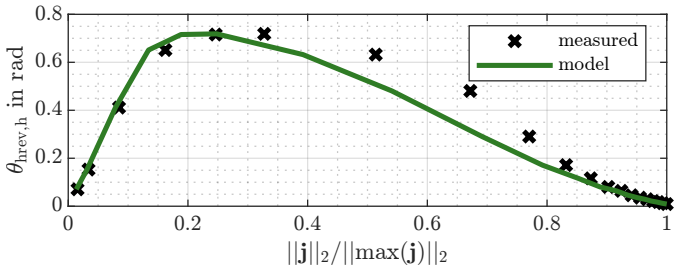

Fig. 8: Comparison between measured and modelled angle between magnetic field strength and the reversible field

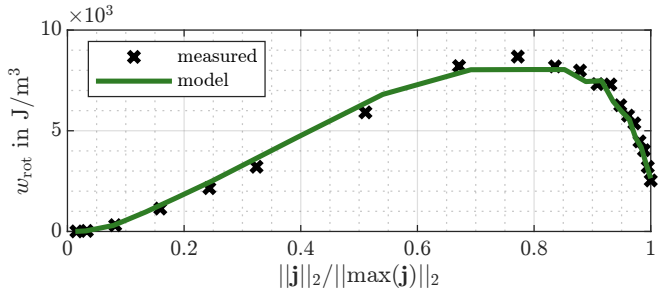

Fig. 9: Comparison between the measured and modelled rotational losses

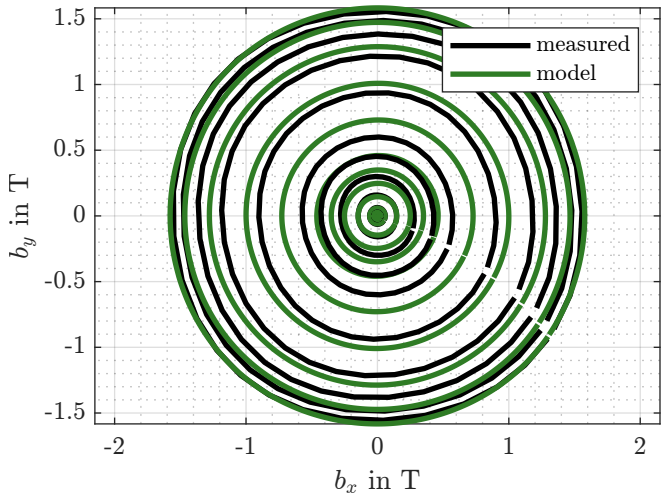

Fig. 10: Comparison between measurements and model results regarding the x-and y-component of the $\boldsymbol{b}$-field

VI. Conclusion

In this paper, the unphysical behaviour of energy-based hysteresis models towards rotational losses is described. To correct this issue, an improvement that adapts the angle between the reversible part of the magnetic field and the total applied magnetic field is proposed by introducing a rotational matrix that rotates the reversible part towards the applied field for high states of saturation. The behaviour of the rotation is governed by an analytical function $f^k(\|\boldsymbol{j}^k\|)$ with parameters to be identified. To choose these parameters, a method is presented that is able to split the measured field into its reversible and irreversible part. This information can be used to obtain the behaviour of the measured angle between the reversible part of the magnetic field and the total applied magnetic field. On the basis of this angle, the parameters can be identified. The results show that for the used soft magnetic material it is possible to correctly adapt the angle and the rotational losses on the basis of the splitting of the measured field quantities. Further, it is shown that the behaviour of the $\boldsymbol{b}$-field also agrees with measurements, with only some minor discrepancies. For future work, this procedure is tested on more materials which can also be anisotropic.

Acknowledgement

The work is supported by the joint DFG/FWF Collaborative Research Centre CREATOR (CRC – TRR361/F90) at TU Darmstadt, TU Graz and JKU Linz.

References

[1] A. Bergqvist, "Magnetic vector hysteresis model with dry friction-like pinning," *Physica B: Condensed Matter*, vol. 233, no. 4, pp. 342–347, 1997.

[2] M. Kaltenbacher, K. Roppert, L. D. Domenig, and H. Egger, "Comparison of energy based hysteresis models," in *2022 23rd International Conference on the Computation of Electromagnetic Fields (COMPUMAG)*, 2022, pp. 1–4.

[3] K. Jacques, "Energy-based magnetic hysteresis models-theoretical development and finite element formulations," 2018.

[4] R. Scorretti and F. Sixdenier, "An analytical formula to identify the parameters of the energy-based hysteresis model," *Journal of Magnetism and Magnetic Materials*, vol. 548, p. 168748, 2022.

[5] V. François-Lavet, F. Henrotte, L. Stainier, L. Noels, and C. Geuzaine, "An energy-based variational model of ferromagnetic hysteresis for finite element computations," *Journal of Computational and Applied Mathematics*, vol. 246, pp. 243–250, 2013.

[6] L. Prigozhin, V. Sokolovsky, J. W. Barrett, and S. E. Zirka, "On the energy-based variational model for vector magnetic hysteresis," *IEEE Transactions on Magnetics*, vol. 52, no. 12, pp. 1–11, 2016.

[7] A. Sauseng, L. Domenig, K. Roppert, and M. Kaltenbacher, "Adaptions of the energy-based hysteresis model for correct rotational losses," in *2022 IEEE 20th Biennial Conference on Electromagnetic Field Computation (CEFC)*. IEEE, 2022, pp. 01–02.

[8] D. Lin, P. Zhou, and A. Bergqvist, "Improved vector play model and parameter identification for magnetic hysteresis materials," *IEEE Transactions on magnetics*, vol. 50, no. 2, pp. 357–360, 2014.

[9] K. Jacques, S. Steentjes, F. Henrotte, C. Geuzaine, and K. Hameyer, "Representation of microstructural features and magnetic anisotropy of electrical steels in an energy-based vector hysteresis model," *AIP Advances*, vol. 8, no. 4, p. 047602, 2018.

[10] T. M. Inc., "Matlab version: 9.13.0 (r2022b)," Natick, Massachusetts, United States, 2022. [Online]. Available: https://www.mathworks.com